Norwegian University
of Life Sciences

Master's Thesis 2021 30 ECTS
Faculty of Chemistry, Biotechnology and Food Science

Microbiota composition and activity at different stages of the HIAS sewage phosphorus removal

Vemun Holmestrand
Chemistry and Biotechnology

Abstract:

Phosphorus contamination from unprocessed sewage causes environmental damages through eutrophication in aqueous ecosystems. Certain biological wastewater treatment plants can remove phosphorus from the wastewater and recycle it for use in agriculture. Enhanced biological phosphorus removal methods employ phosphorus accumulating microbes in biofilms to remove phosphorus from sewage. Hias wastewater treatment plant's Hias process has shown efficient phosphorus removal and recycling, however, the microbiological function of the process is not well understood. The main aim of this study is to analyze the microbial composition on the biofilm carrying the phosphorus accumulating organisms and changes to the microbiota through the Hias process. To investigate the process, biofilm samples were taken from anaerobic reactor 3, and aerobic reactors 5 and 10. DNA and RNA is extracted using a MagMAX 96 total RNA isolation kit. The nucleic acid content of the samples was sequenced using Illumina.

The sequencing showed phosphorus accumulating organism genera *Tetrasphaera* and *Candidatus Accumulibacter* in high abundance. The nitrifying and ammonium oxidizing bacteria genera of *Nitrosomonas* was present at high abundance. The most abundant genera in the data set is *Uncultured Saccharibacter*. The experimental procedure yielded low concentrations of nucleic acid. This led to statistical uncertainties which made potential biological inferences regarding the microbial community uncertain. This paper then goes into potential improvements on efficiency of the experimental protocol, with regards to nucleic acid extraction from the biofilm. Further work is needed to properly assess the correlations between RNA levels in different reactors.

Keywords:

- **AS:** Activated sludge
- **EBPR:** Enhanced biological phosphorus removal
- **EPS:** Extracellular Polymorphic Substance
- **GAO:** Glycogen Accumulating Organisms
- **MBBR:** Moving Bed Biofilm reactor
- **OTU:** Operational taxonomic unit
- **PAO:** Phosphorus Accumulating Organisms
- **PHA:** Polyhydroxyalkanoate
- **VFA:** Volatile fatty acid.
- **WWTP:** Wastewater treatment plant

1. Theory:

1.1 Phosphorus

Phosphorus is an essential element to all life. It has key roles in the structure and function of important cellular constituents like nucleic acids, adenosine triphosphates and phospholipids. Aside from nitrogen, phosphorus is the primary limiting nutrient to the growth of organisms (Ruttenberg, 2003). Mass scale agriculture is for that reason dependent upon phosphorus-based fertilizer. More food is needed to sustain a continuously growing human population, alongside higher standards of living. Phosphate is supplied as fertilizer through phosphate rock. Phosphate rock is a non-renewable resource (Ruttenberg, 2003).

Current use of phosphorus also poses environmental issues. Eutrophication is the process in which large amounts of micronutrients in aqueous ecosystems cause algal bloom. As use of phosphorus fertilizers keep increasing, so does the stress on proximal environments susceptible to eutrophication (Bhagotwati, 2018). Rain and erosion bring phosphorus to lakes and rivers from agricultural landscapes. Sewage contains phosphorus through human waste and wastewater treatment plants (WTTP) release effluent waters into these aqueous ecosystems. Release of phosphorus rich wastewater promotes algal growth and toxic algae can destroy ecosystems in lakes and reservoirs for drinking waters (Bhagowati, 2018). Technologies for recycling usable phosphorus is for these reasons important for environmental sustainability.

1.2 Sewage processing

Unprocessed sewage contains high amounts of phosphorus from human waste and can therefore pose a threat to local environments. Wastewater treatment plants (WWTPs) are run to follow environmental regulations, such as discharge limits on phosphorus and nitrogen to prevent eutrophication (Bhagowati, 2018). There are multiple steps in and ways to treat wastewater to become safe for the environment. Mechanical separation is used to filter out solids from the water. Even still, many nutrients and dissolved contaminants remain. One way to remove phosphorus specifically is through chemical separation. Using multivalent metallic ions, such as iron and aluminum, one can precipitate phosphate through binding with the metal. The metal-phosphorus precipitate can then be mechanically removed from the waters. Phosphate bound this way is difficult to separate from the metallic cations. This results in low degree of bioavailability, making it a poor fertilizer (Bunce, 2018) (Lenntech, 2021).

Biological phosphorus removal in wastewater treatment is a viable alternative to chemical precipitation. Biological phosphorus removal is based on microbes using phosphorus as a substrate and store it in a biomass. Mechanically separating the microbial biomass, the phosphorus can be both removed from wastewater and potentially be reused in agriculture. Enhanced Biological phosphorus removal (EBPR) in WWTPs were developed to accommodate for this (Saltnes, 2017) (Bunce, 2018).

1.3 Enhanced biological phosphorus removal

EBPR processes are based on activated sludge methods. Activated sludge (AS), is a microbially based biomass containing various bacteria that can use nutrients in wastewater as substrates. The AS process is a loop that consists of an aeriation tank, a settler, and a return pipe for sludge (Hreiz, 2015). Phosphorus accumulating organisms (PAO) in the AS assimilate phosphorus as polyphosphate chains aerobically. Influent water is mixed with recycled AS from the return pipe before entering the aeriation chamber. Phosphorus is fixed into the AS in the aeriation chamber. In the settler, the AS is separated from the water through gravity sinking the sludge to the bottom. The sludge is brought back through the return pipe and applied back to the influent water for reuse. Excess sludge is brought out of the system through a sludge deposit pipe along with phosphorus bound in the PAOs in the AS (Hreiz, 2018) (Lenntech, 2021). A schematic representation of this process is described in figure 1.

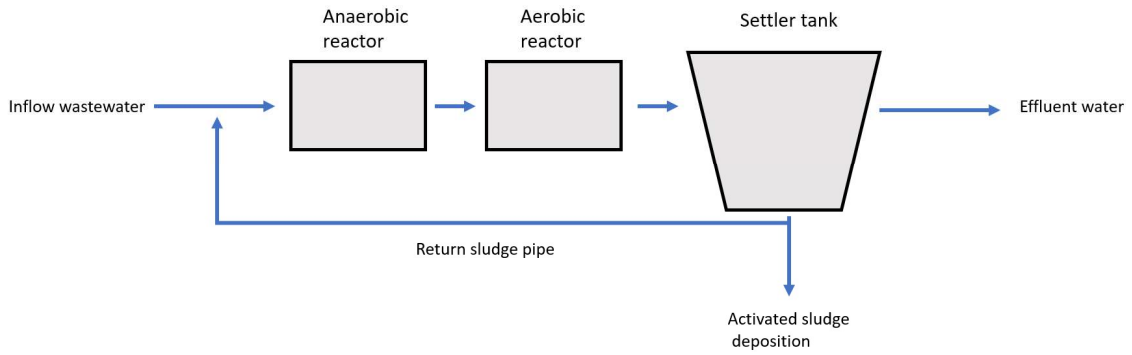

Figure 1: Adapted from Lenntech, 2021. Diagram of AS system EBPR, showing the flow of wastewater and the different treatment steps. Wastewater is introduced to the system and mixed with return sludge. The mixture is introduced into the anaerobic chamber, then the aerobic chamber, then the settler tank. AS is separated from the wastewater in the settler tank and goes on to become effluent. Some sludge is deposited, the rest is recycled back with the influent water.

Modern and more efficient ways to conduct EBPR has been developed since but are still based on this principle. One of these technologies is the Moving bed biofilm reactor (MBBR). MBBR is based on wastewater flow through sequential aerobic- and anaerobic tanks. The reactors are constantly stirred to cycle the biofilm carriers through the entire volume of the tank. The advantages of MBBR compared to EBPR systems is better performance degrees over smaller volumes, increased resistance to environmental changes, and no recirculation of sludge, which causes clogging (Di Biase, 2019) (Rusten, 2006).

1.4 Phosphorus accumulating organisms.

As technology and knowledge surrounding molecular biology improves, biological removal of phosphorus in wastewater treatment has become better understood and the species of bacteria that preform phosphorus fixation have been sequenced. Using this information, engineering microbial communities for better removal of nutrients from wastewater is possible. *Candidatus Accumulibacter*, *Tetrasphaera*, *Dechloromonas*, *Microlunatus*, *Phosphovorus*, *Tessaeacoccus* and *Candidatus Obscuribacter* are all important PAO genera (Roy, 2019).

Candidatus Accumulibacter has been used as an organism of study for poly-P storage and use in EBPR. *Candidatus Accumulibacter* will in anaerobic conditions take up carbon-based nutrients in the environment such as volatile fatty acids (VFA) like acetate. The polyphosphate reserves in the PAO are broken down and energy is released in form of ATP. This energy used for breaking down the VFA. The orthophosphates (PO_4^{-3}) that are cleaved off from the poly-P reserve are released into the environment. Glycogen in the cell is catalyzed to pyruvate which reacts with the catabolized VFA to become Acetyl-coA, which in turn is catalyzed into polyhydroxyalaknoates (PHA) (Tarayre, 2016).

Candidatus Acummulibacter use orthophosphates in the environment in effluent water during aerobic conditions and store them by binding them in the Poly-P reserves. By catabolizing PHA, using oxygen gas as the terminal acceptor, the PAO fixate orthophosphate as a monomer to Poly-P in the polyphosphate reserves. PHA reactions are also used by the cell to replenish glycogen and for cell growth. Phosphorus accumulation is based on access to oxygen, pH, temperature, volatile fatty acid composition, concentrations of PO_4^{3-}, SO_4^{2-}, NH_4^+, K^+, Na^+, Mg^{2+}, Ca^{2+}, and other metal ions. (Bunce, 2018) (Tarayre, 2016) The mechanical workings of phosphorus fixation and dissociation processes are described in figure 2.

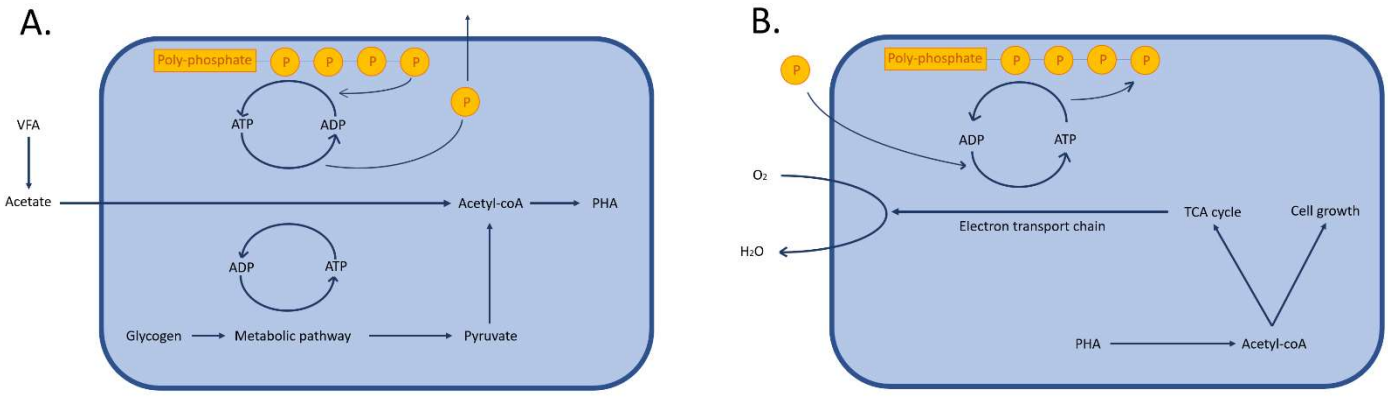

Figure 2: Adapted from Tarayre, 2016 and Bunce 2018. Shows the biochemistry of Poly-P catabolism and anabolism in *Candidatus Accumulibacter*. Under anaerobic conditions (A), an environmental carbon source is used to break down the polyphosphate chains and build up PHA. VFAs as acetate is converted to actyl-coA through breaking down glycogen stores and poly-P. The pyruvate resulting from glycogen breakdown reacts with acetyl-coA and forms PHA. Free orthophosphates are released to the environment. In aerobic conditions (B), polyphosphate is

built up by breaking down PHA and consuming oxygen gas. PHA is broken down to acetyl-coA, used to fuel the TCA cycle. Through the electron transport chain, free orthophosphate molecules are incorporated into the poly-P storage. O_2 is the terminal acceptor of the electron transport chain.

1.5 Other functional bacterial groups in EBPR

While PAOs are needed for the functioning of EBPR, other microbes are also necessary. A study revealed the relative ratios between functional groups of microbes in EBPR systems in Denmark (Nielsen, 2010). On average, 28% of bacteria were filamentous hydrolyzers, 18% were denitrifiers, 13% were PAOs, 7% were nitrifiers, 3% were hydrolyzers, 3% were fermenting bacteria, and 1% were GAO. The remaining 23% were other functional groups and microbes of unknown Operational Taxonomic Unit (OTU).

Influent wastewater contains macronutrients inaccessible to the functional PAOs or denitrifying organisms. Hydrolyzing bacteria use enzymes to break down macronutrients to oligomers or monomers that functional bacteria can use. There is overlap between hydrolyzing OTUs and other categories and groups. (Nielsen, 2010) PAOs can also hydrolyze substrates, such as *Tetrasphaera* which hydrolyzes polysaccharides into glucose, which is used by several OTUs like *Candidatus Accumulibacter*. Filamentous bacteria are an abundant type of bacteria that conduct various forms of hydrolysis. *Microthrix* can break down lipids to glycerol, and *Saccharibacter* break down peptides to amino acids. Filamentous *Streptococcus* species is an example of a fermenting bacteria, anaerobically breaking down glucose. Fermenting bacteria are responsible for VFA formation (Nielsen, 2010)

Bacteria that use nitrogen for respiration are useful for removing nitrogenous substrates from wastewater. Selecting for these bacteria in WTTP systems can therefore be useful. Ammonia oxidizing bacteria turn ammonia to nitrite, nitrite oxidizing bacteria turn nitrate to nitrate, and nitrate reducing bacteria turn nitrate to nitrogen gas (Seifi, 2012). When conditions are right, these functional bacteria can all operate at once. This is called simultaneous nitrification and denitrification (SND). SND in EBPR systems allows denitrifying PAOs (DNPAO) to use the same energy source for assimilating orthophosphate and denitrify (Oehmen, 2007). This results in efficient removal of phosphorus and nitrogen.

When engineering microbial communities for the sake of EBPR, one must account for competitors like Glycogen Accumulating Organisms (GAO). GAOs cycling of glycogen is like PAOs cycling of PHA, but GAOs do not store orthophosphate. Low abundances of GAOs in EBPRs are associated with lower concentrations of phosphorus in effluent water from processing plants with EBPR. Examples of GAO are *Competibacter*, *Contendibacter* and *Defluviicoccus* (Roy, 2021). One way to create unfavorable conditions for GAO are through water temperatures lower than 20°C (Nielsen, 2010).

In a MBBR process, all the microbes are attached to biofilm carriers through the biofilm. A biofilm is a matrix microbial ecosystem bound together with cells and extracellular polymorphic substances (EPS). Cells in the biofilm create the proteins and carbohydrate that constitute EPS to replenish it. The biofilm can protect individual cells from environmental dangers, such as protozoans, inhibitors, or dehydration. A biofilm is complex and heterogenous, with different species of microbes in different parts of it. In

aerobic environments, aerobic bacteria are found most on the surface of the biofilm, whereas the anaerobic ones are found deeper within (Di Biase, 2019) (Donlan, 2002).

1.6 Hias process

In the 1970s, cyanobacteria started growing on Mjøsa, a lake in Innlandet, Norway. The drinking water supplied from there became contaminated as a result. Diagnostics showed the cyanobacteria bloom was a part of eutrophication resulting from phosphorus release into the water from the region. The Mjøsa campaign was launched to save the lake through reducing phosphorus contamination from sewage and agriculture (Norwegian Ministry of environment, 1979) (Bechmann, 2021). The Hias WTTP made an AS system for biological removal of phosphorus in 1974 (Hias, 2021).

Hias is the WTTP for the municipalities Hamar, Løten, Stange and Ringsaker in Innlandet, Norway and releases water into Mjøsa. The sewage processing takes place over three steps: mechanical, chemical, and biological. The upgrade to their biological wastewater treatment finished development in 2016 and is called the Hias process. It is based on MBBR and activated sludge systems with SND. This treatment step can recover as much as 50% of phosphorus in a reusable from (Hias, 2021).

The process uses biofilm attached to biofilm carriers taken through aerobic and anaerobic/anoxic chambers. As seen in figure 3, the process is split into 10 reactors, where the first 3 are anaerobic, the next 7 are aerobic. The biofilm carriers used are 0.95 g/cm^3 polyethylene K3 Kaldnes biofilm carriers (Rusten, 2006). The biofilm carriers are by the end of the process separated from the wastewater and excess sludge and transported back into the first reactor through a lift. The excess sludge containing the phosphorus is separated from the water and later processed to become struvite-based fertilizer. The remaining effluent is processed one last time through a tertiary treatment to meet the 0,4 mg/L discharge limit requirement (Saltnes 2017).

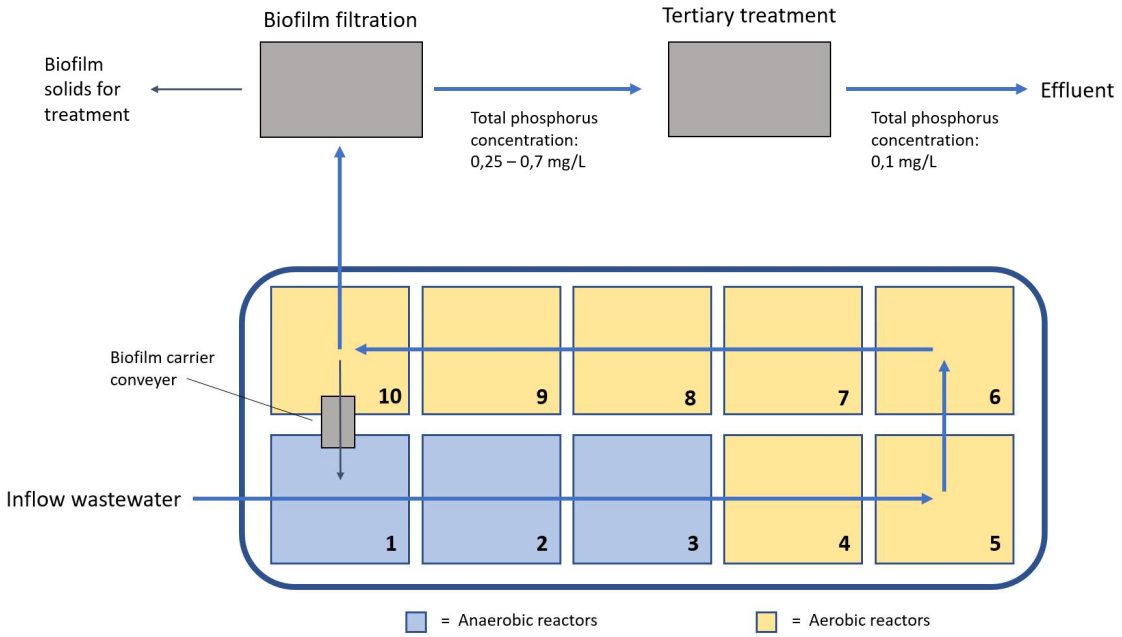

Figure 3: Adapted from Hias.as, 2021. Schematic representation of the Hias process. The reactors are numbered by order. Wastewater is introduced to the biological wastewater treatment in reactor 1. Here the recycled biofilm carriers are introduced to the wastewater. The water is put through 3 anaerobic MBBRs, then 7 aerobic ones. In reactor 10, the biofilm carriers are lifted out of the sewage and transported back to reactor 1. The wastewater is transported to a biofilm filtration chamber, where the biofilm solids are separated from the wastewater. The water goes through a tertiary treatment before being released into Mjøsa.

1.7 Molecular techniques

To analyze nucleic acids from cells in a biofilm, the cell walls and biofilm must be broken down and separated. The nucleic acid extraction is the first step in the nucleic acid isolation that leads to analysis through sequence analysis and quantification. Cell walls and biofilms can be destroyed through mechanical shear force, such as bead beating, or chemicals or enzymes that dissolve intramolecular or intermolecular bonds. Considerations are important when extracting RNA. Environmental RNases can break down RNA during and after the nucleic acid extraction. Using RNase blockers like RNase away can prevent RNA degradation (Green, 2019).

The process of nucleic acid isolation begins with the extraction. Nucleic acids can be bound to magnetic beads through their net negative charge. Using this, other molecules can be washed away using wash buffers. Several different wash buffers are commonly used and multiple times per sample. Freeing nucleic acids from the magnetic beads is done after the washing steps. This is done using an elution buffer. RNA samples are made using DNase treatment on those samples (Invitrogen, 2018).

rRNA levels in cell abundance can be compared to DNA abundance from the same species to determine relative expression levels. The levels of nucleic acids can be determined through sequencing of the

samples or through qPCR. rRNA abundance can be measured through synthesizing cDNA from the rRNA. Expression levels can then be determined through comparing DNA and RNA levels with cDNA levels. cDNA is DNA synthesized from reverse transcriptase. The reverse transcriptase enzyme binds to RNA and using it as a template, makes copy DNA (cDNA). The cDNA can then be used in sequencing (Pray, 2008).

Annotation, taxonomic analysis, and microbial diversity in the biofilm can be examined through nucleic acid sequencing. High through put next generation sequencing technology, such as Illumina, can annotate isolated nucleic acids through 16S rRNA sequencing. 16S rRNA genes from the library is ligated with primers, then sequenced. cDNA synthesis through reverse transcriptase will also allow quantification of relative amounts of different microbes (Pray, 2008). Metagenome data from the sequencing can be further processed using a bioinformatics pipeline like QIIME. QIIME processes the sequences through "Demultiplexing, quality filtering, OTU picking, taxonomic assignment, phylogenetic reconstruction, diversity analysis" (Caparaso, 2010).

Illumina sequencing starts with library preparation. DNA fragments are ligated with adapters. The adapters are complementary to oligonucleotides in the Illumina flow cell lanes. The dsDNA is cleaved to yield ssDNA. A complementary sequence to the ssDNA strand is synthesized using polymerase. The newly synthesized dsDNA binds to complementary oligonucleotides on the flow cell surface. The newly synthesized complementary strand and the original strand are cleaved. This cycle repeats until the flow cell is filled with clones of the same strand. The ssDNA is read and sequenced using fluorescent DNTPs sequentially binding to the clone DNA strands (Buermans, 2014).

1.8 Aim of the study

The Hias process is not well understood microbiologically. Using molecular approaches, species of microbes and their relative abundance and substrate dependance can be identified. This could help further improve the phosphorus removal efficiency of the Hias process. Understanding the microbial community could lead to it being further engineered, or the process adjusted, to optimize the utility of the bacteria involved. Part of this process is through comparing abundance of DNA and RNA of the microbes in the community between the aerobic- and anaerobic chambers of the Hias process to determine which microbes are present and expressed under which conditions. To accomplish this, isolated nucleic acids and rRNA in the form of cDNA will undergo metagenome sequencing.

The primary aim of this study is to analyze the composition of and changes in microbiota across the Hias process. The aim will be accomplished through the following sub-goals:

- Device a protocol for nucleic acid extraction based on the biofilm carrier medium.
- Optimize the protocol for higher RNA and DNA yield.
- Comparing relative abundance changes in transcription levels of bacteria between the aerobic chambers and the anaerobic chambers of the Hias process.
- Comparing relative abundance changes in transcription levels of bacteria with their biology.

Insight into experimental process optimization will be gained through gel electrophoresis assays and eventually qPCR determining the amount of nucleic acid present.

2. Materials and methods:

The test material collected are the biofilm carriers used in the Hias process. Biofilm carriers will be analyzed from reactor 3, which is anaerobic, and reactors 5 and 10 which are aerobic. The nucleic acids will be recovered through lysis and isolation. cDNA synthesis will be used to determine the level of expression through 16S rRNA levels at the different reactors. Relative abundance of microbes in the community will be determined through metagenome sequencing. Figure 4 summarizes the sample processing in this thesis. Table 1 summarizes the parameters of the process optimization that lead to the approach seen in figure 4.

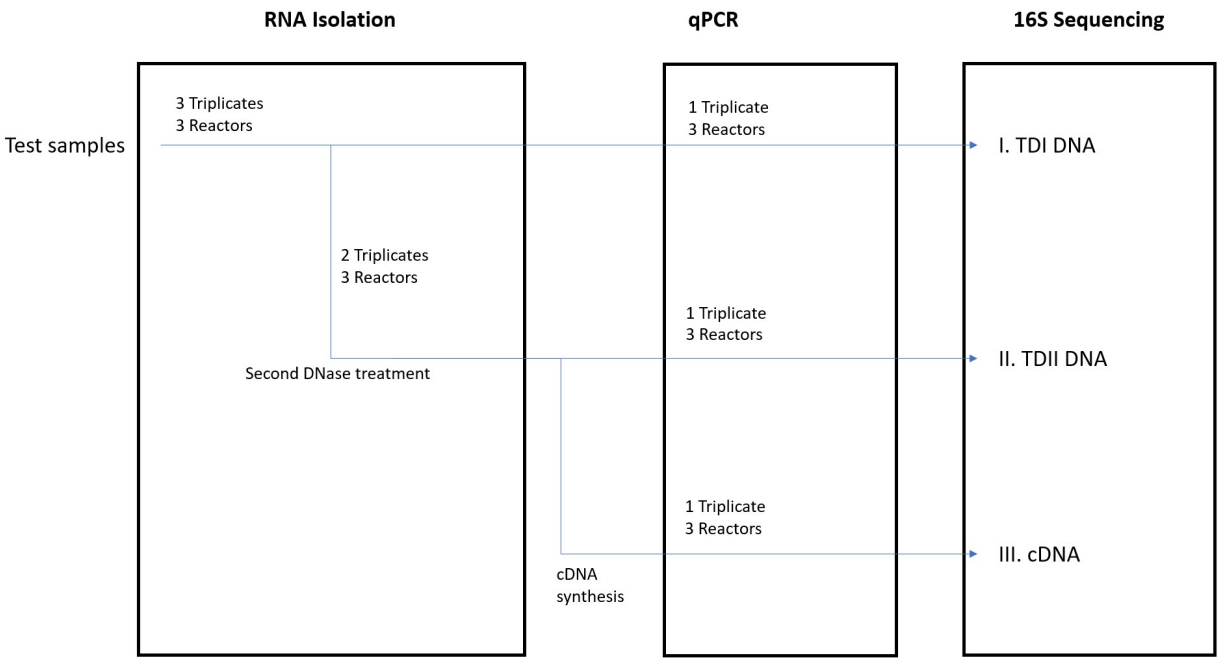

Figure 4: Flow-chart of test samples through the procedure of the materials and methods. The 3 triplicates of each of the three reactors were split off at junction points. The first is where 2 of the 3 triplicates is treated with Turbo DNase again. The second is where 1 of the 2 triplicates is used to synthesize cDNA. Each of the triplicate sets are analyzed by 16S sequencing. The execution of the method as described in the Materials and Methods segment, as well as initial qPCR assay and sequencing and pipeline work was done by Inga Leena Angell.

Table 1: Summary of parameters for the protocol optimization across test runs. The five-pilot procedure runs and the final run from where the results were produced are accounted for. The table accounts for which nucleic acids were being tested for in the different runs, the nucleic acids present for the assay, the amount of sample material used, the presence of positive controls and the form of shearing lysis used on the sample materials.

	Tested for	Nucleic acid presence	Sample material	Positive control	Shearing
Test run 1	DNA	DNA	3, 2 & 1 spoke pieces		FastPrep96
Test run 2	RNA & positive control	Positive control only	1 spoke pieces	Yes	None
Test run 3	RNA positive control	Positive control only	1 spoke pieces	Yes	Centrifuge
Test run 4	RNA & positive control	RNA (degraded)	1 spoke pieces	Yes	MagNa lyser
Test run 5	DNA, RNA and positive control	DNA	½ spoke pieces	Yes	MagNa lyser
Final protocol	DNA, RNA & positive control	DNA, RNA (qubit)	½ spoke pieces	Yes	MagNa lyser

2.1 Material Collection:

Four Falcon Tubes filled with 30 mL RNA later were brought from the Norwegian University of Life Sciences to the Hias Wastewater treatment plant in Hamar. Six K3 Kaldnes biofilm carriers were taken from reactor chamber 3, 5 and 10 in the MBBR, and placed into respective Falcon tubes. Six more biofilm carriers from reactor chamber 5 were stored in the last Falcon tube and were used as pilot samples for the experimental approach. The samples were gathered 8th of January 2021 at approximately 13:15 and were deposited in a - 20°C freezer at NMBU approximately 15:30. The biofilm carriers were stored in an upright position with RNA later covering all the biofilm carriers for the duration of the trip. The gathering of biofilm carriers within the plant was done by one of the plant operators.

2.2 RNA isolation:

For the procedure, 32 samples were prepared. 27 from the biofilm carriers, 4 negatives and 1 positive control. The samples are divided by reactor, so 9 samples for reactor 3, 9 for reactor 5, and 9 for reactor 10. All mixing of reagents was done with a 10% overage in this paper.

The Falcon tubes were taken out of the freezer. The biofilm carrier samples thawed on the bench. A box of ice was prepared. The chemicals for RNA isolation are found in the MagMAX 96 Total RNA kit. It was made sure the concentrates were added the appropriate solvents as described in the kit's description before use (6 mL 100% isopropanol to the wash solution 1 concentrate, 44 mL 100% ethanol to wash solution 2 concentrate and 6 mL isopropanol to RNA binding concentrate). RNA binding beads were thawed on the bench, then the tube of beads was vortexed for a few seconds. 10 µL vortexed RNA

binding beads were mixed with 10 µL lysis/binding enhancer in a microtube for every sample. The solution was mixed by pipetting, then put in the freezer box.

63 µL 100% isopropanol was mixed with 77 µL lysis/binding solution in a tube for each sample. The tube with the mixture was stored in room temperature.

After the biofilm carrier samples were thawed, the tubes were put on ice and RNase away was applied to a sterile scalpel. One of the biofilm carriers were put on a sterile petri dish with RNase way. The biofilm carriers were cut to a one-spoke piece from around the outer ring. Then the one-spoke pieces were cut in half across the circumference of the piece. Pieces were cut until 9 half-spoke pieces for each of the 3 reactors were ready. This yielded three half spokes per reactor per three treatments (3 Triplicates per 3 reactors, equals 27 samples).

140 µL of the already mixed lysis/binding solution were added to each of the tubes with the biofilm carrier pieces. 30 µL of a positive control solution was added to one tube, and 30 µL of nuclease free water was added to 4 2mL tubes as negative controls. Then the 140 µL of lysis/binding solution mix was added to each of those. All the samples and control tubes were put on the MagNa lyser shaker for 40 seconds, 2 times with a minute between at 6000 rotations per minute (rpm).

The RNA binding bead mixture was vortexed and then 20 µL of the mixture was applied to each of the samples and controls. Every sample was put on an orbital shaker for 5 minutes at 1250 rpm. Then the tubes were put onto a magnet stand for 3 minutes. The supernatant was pipetted and discarded. Then the tubes were removed from the magnetic stand, and 150 µL wash 1 buffer was applied to each of the tubes. The biofilm carrier pieces were discarded without disturbing the magnetic beads. The tubes were put on an orbital shaker at 1250 rpm, 1 minute. The tubes were put on the magnetic stand for 2 minutes. The supernatant was discarded without disturbing the beads, then the tubes were taken off the magnetic stand.

150 µL wash 2 buffer was applied to each tube. The tubes were put on ice. 49 µL MagMAX turbo DNase buffer was mixed with 1 µL turbo DNase for each tube. The solution was mixed by pipetting. The tubes were taken from the ice and put on orbital shake at 1250 rpm for 1 minute. The tubes were put on the magnetic stand for 2 minutes. The supernatant was discarded, then the tubes was taken off the magnetic stand. 50 µL of the DNase buffer was applied to each of the tubes. The tubes were put on the orbital shake for 15 minutes at 1250 rpm. 50 µL of RNA rebinding solution was applied to each tube. Samples were orbital shaken for 3 minutes at 1250 rpm. The tubes were put on a magnetic stand for 2 minutes. The supernatant was discarded, then the tubes removed from the magnetic stand.

150 µL of wash 2 buffer was applied to each sample and the tubes shaken on the orbital shaker for 1 minute at 1250 rpm. The tubes were put on a magnetic stand for 2 minutes, then the supernatant discarded, and the tubes from the stand removed. This step was repeated from wash 2 buffer application. After discarding the supernatant, the tubes were put on the orbital shaker for 2 minutes without the lid on. 50 µL elution buffer were applied to each tube. The samples were orbital shaken for 3 minutes at 1250 rpm. The tubes were put on a magnetic stand for 3 minutes. The elution was pipetted

over to new tubes without disturbing the magnetic beads. The Ambion Turbo DNA-free Kit was used on two of the three triplicates for each reactor. The elution was put on ice.

2.3 Gel screening:

One gram of agarose was mixed with 50 µL TAE×1 buffer and 2 µL peqGREEN in a flask that could withstand microwaving. The flask was put in a microwave oven, then the flask was sequentially heated and shaken until the solution become transparent with no floating particles. The flask was put aside while cooling.

The gel tray and well comb was washed with RNase away. 10 µL of the elution was applied from each triplicate into a new tube and mixed with 2 µL ×6 loading dye using the pipette. After the agarose gel had cooled to where it would soon solidify, the content was poured into the gel tray with the well comb in. After the gel was solidified the comb was removed. The gel was put in the electrophoresis vat with the wells on the negative side. The vat was filled with TAE×1 buffer until the gel was covered.

3 µL of 100b ladder was applied to one well and the elution loading buffer mixes to the others. The electric current was turned on for 30 minutes on 80 volts. After the gel has been run, the gel was analyzed through UV fluorescent computer screening on GELdocXR.

2.4 cDNA synthesis:

On a PCR strip, one of the triplicates from each reactor that underwent the second DNase treatment was applied. 10 µL per sample was taken from each tube. For each of the tubes, 2 µL RT reaction premix with random primers, 1.5 µL FIREscript enzyme mix and 6.5 µL nuclease free water was applied and mixed by pipetting. The samples were incubated for 10 minutes.

A heating block was programmed to follow this sequence: 1 hour at 50°C, 5 minutes at 85°C and then cool to 4°C. After the incubation, the PCR strip was run on the program to synthesize cDNA. After cooling off, the cDNA was put away on ice.

2.5 Quantitative Polymerase Chain Reaction:

Qubit dsDNA HS 200× was diluted using Qubit dsDNA HS buffer in a 1:200 relation. 10 µL of standard solution 1 and 2 was applied to each their own qubit tube with 190 µL of the diluted Qubit dsDNA HS buffer dilute. 2 µL of each of the 3 triplicates for the 3 reactors was applied in each their own qubit tube and mixed with 198 µL of the diluted Qubit dsDNA HS buffer dilute. The tubes were vortexed for 3 seconds. The tubes were incubated for 2 minutes. The Qubit fluorometer was calibrated using the standard solutions. The DNA concentrations were read given 2 µL adjustment on the fluorometer.

4 µL 5× HOTFIREPol EvaGreen qPCR supermix, 0.4 µL forward primer PRK341F, 0.4 µL reverse primer PRK806R, and 14,2 µL nuclease free water was mixed for each sample and control. Based on the Qubit

results, any solution with nucleic acid concentration higher than 10 ng/µL was diluted to be lower than 10 ng/µL. 19 µL of the qPCR mix were applied to wells in a qPCR plate for every sample and control. 1 µL of the nucleic acid elution was added to each their own well. 9 samples treated once with DNase, 9 samples treated twice with DNase, and 9 samples treated with DNase twice, then cDNA synthesized.

The lid on the qPCR plate was put on. The plate was spun on a 'mini plate spinner mps1000', with a counterweight. The spinner was run until it reached max speed. The qPCR plate was put on a qPCR machine with the following program coded: 95°C for 15 minutes, then repeat these three steps 40 times: 95°C for 30 sec, 55°C for 30 sec, 72°C for 45 sec.

2.6 Sequencing:

The 27 samples, the 4 negative controls and the positive control that were analyzed in the qPCR procedure were sent off for 16S V3 V4 sequencing. The sequencing technology used is Illumina. The procedure of sequencing is as described in Rudi, 2018. The sequences were preprocessed through the QIIME pipeline for demultiplexing and primer truncation. The bioinformatics processing produced diversity plots, relative abundance charts and tables, phylogenetic trees and OTU annotations of the different samples' sequences. These data were statistically analyzed for results and discussion purposes. The results were categorized by the different reactors the initial sample was taken from, as well as whether the sample had been treated with Turbo DNase once or twice or if it was cDNA.

3. Results:

3.1 Process optimization

Figure 5 summarizes the optimization process for the five iterations of the experimental protocol. Results of the protocol optimization showed variable amounts of DNA and RNA, with the first test run showing DNA presence, the second and third showing small amounts of RNA in positive controls, the fourth show some RNA in the test results and the fifth with DNA.

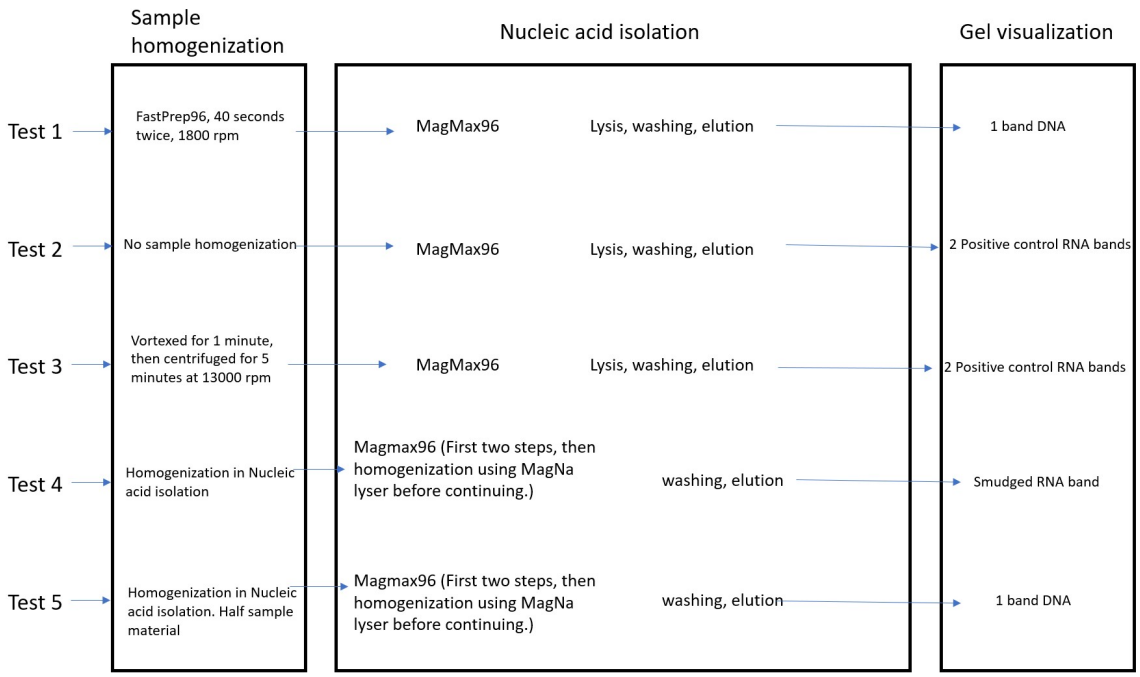

Figure 5: Flow chart of the optimization test runs executed. The 5 test runs are sequentially run through a step of sample homogenization, then nucleic acid isolation, then gel visualization. The different test steps are described with the procedures that took place under the different stages of optimization testing.

For the first test run, the biofilm carrier was initially cut into three-, two- and one-spoke pieces. Each of these would be run as parallels through the first iteration of the protocol. FastPrep96 was used for shearing the biofilm for this first iteration, 40 seconds twice at 1800 rotations per minute. The RNA isolation protocol had no DNase treatment step and had no MagNa lyser process. From the gel electrophoresis as seen in figure 6 (A), The first run shows DNA present in the sample. The bands have a low degree of clarity, indicating low amounts of DNA or high degrees of degradation. The four wells marked were the 1 spoke and 2 spoke wells, the 3 spoke wells barely shows any bands.

The next test run looked to be increasing nucleic acid yield through stronger cell-lysis. To test for RNA, the shearing step was cut out for the second run of the procedure and the first DNase treatment step was added for one parallel of samples. A positive *Escherichia coli* control was also added as a reference for checking the procedure. The biofilm carrier piece's size did not seem to matter for nucleic acid yield to any noticeable degree, so one-spoke pieces was used for convenience's sake. The second run shows RNA through the positive control lanes on the gel in figure 6 (B). The two bands (16S and 18S) signify RNA and show that the procedure outside the homogenization has been successful. The bands have low degree of clarity, suggesting low RNA levels.

For the third run, adjustments to homogenization were needed as neither the sample RNA nor DNA were visible. The one-spoke pieces were to be vortexed for 1 minute, then centrifuged for 5 minutes, 13000 rotations per minute for homogenization. This did not yield any visible RNA when analyzed on the gel electrophoresis. The two RNA bands as seen in figure 6 (C) are clearer than those in figure 6 (B),

hinting at a better procedure and more nucleic acid content. However, outside of this positive control, no bands for sample RNA nor DNA were perceivable.

The fourth test procedure implemented the MagNa lyser step and the first DNase treatment for one parallel. This procedure gave visible RNA yield on the gel electrophoresis analysis as seen on figure 6 (D). The smudged RNA band hint at RNase contamination or too much sample cell material. The single band makes it look like DNA, but it is the DNase treated sample. The smudged band show a high degree of clarity. The positive control did not show any clear or visible bands. The fifth run was therefore performed with half-spokes instead of whole ones. Figure 6 (E) shows single bands, DNA.

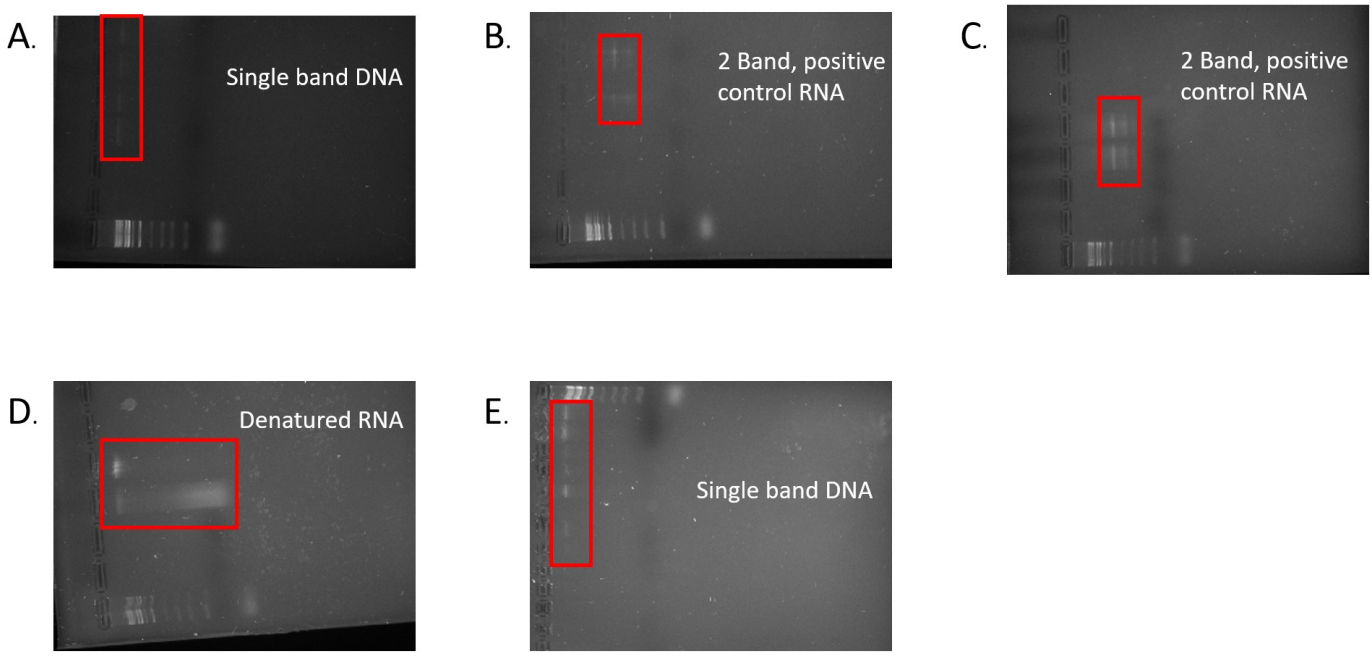

Figure 6: Gel electrophoresis visualizations of the protocol optimization test runs. Shows test run 1 (A), test run 2 (B), test run 3 (C), test run 4 (D) and test run 5 (E). Each are annotated based on observed nucleic acid bands. The ladder used is a 100b ladder. Single band DNA is shown in (A) and (E), positive control RNA is shown in (B) and (C), and denatured sample RNA in (D).

3.2 Results for main experiment

3.2.1 Concentrations of nucleic acids:

With the experimental protocol worked out, the last test-run was performed with parallels for all reactors, with single and double DNase treatment. The tests treated twice with Turbo DNase were used for cDNA synthesis, which was to be used alongside the other samples in a qPCR analysis. Concentration

of samples was determined by Qubit analysis. qPCR was run and results analyzed. The Qubit measured concentrations of nucleic acids in the different tests are displayed in table 2.

Table 2: Qubit measurements of nucleic acid concentrations (ng/µL), across all parallels of all samples, RNA treated once and twice with DNase, and cDNA. Each reactor has one triplicate for every reactor and treatment. The results with insufficient amount of nucleic acid to be detected are labeled with '*Below detection*'.

Sample	**3I**	**3II**	**3III**	**5I**	**5II**	**5III**	**10I**	**10II**	**10III**	**Neg**
RNA (1xDNase)	2.5	2.5	1.4	*Below detection*	4.0	2.0	4.0	2.7	3.1	*Below detection*
RNA (2xDNase)	0.8	0.6	0.3	0.8	0.4	1.0	0.8	0.4	0.6	*Below detection*
cDNA	*Below detection*	*Below detection*	*Below detection*	*Below detection*	*Below detection*	*Below detection*	*Below detection*	*Below detection*	*Below detection*	*Below detection*

The qubit measurements show generally lower concentrations of nucleic acids in the samples that were treated with turbo DNase twice (TDII). The exception is 5I, which had no reading. The cDNA measurements all came below the measurement threshold. The samples only treated with DNase once (TDI) had an average concentration of 2.8 ng/µL, and TDII had an average of 0.63 ng/µL.

3.2.2 Taxonomic analysis

The sequenced 16s rRNA genes are ordered taxonomically after phylum, class, order, family, and genus. The taxonomic analysis on a class level after a 16s sequencing of the samples. Among the abundant phyla are *Clostridia*, *Saccharibacteria*, *Betaproteobacteria* and *Sphingobacteriia*. Figure 7 summarizes the relative amounts of OTUs at class level, as well as showing the different reactors and treatments' relative amount.

The most common phyla are *Actinobacteria* at 31.0% relative abundance, *Firmicutes* at 24.1%, *Proteobacteria* at 20.6% and *Saccharibacteria* at 14.8%. There are 30 phylum OTUs described in the dataset. There are 73 class OTUs. *Actinobacteria* is most abundant at 29.8%, then *Bacilli* at 16.8% and *Betaproteobacteria* at 8.9%. *Actinobacteria* and *Bacilli* are both common in the negative control at an average abundance of 36.1% and 50,5% respectively.

At order level there are 132 OTUs. The most abundant order is *Micrococcales* at 29.1% relative abundance. Second most abundant is *Bacillales* at 14.2% and third is the *uncultured Saccharibacteria* at 9.5%. There are 248 family OTUs. *Bacillaceae* is most abundant at 14.1%, then *Microbacteriaceae* at 13.3% and *Micrococcaceae* at 10.2%. At genus level, there are 547 OTUs. *Uncultured Saccharibacteria* has a 9.5% abundance across all parallels and was the most abundant non-negative-control genus. *Tetrasphaera* is present at 5.2%, *Candidatus Accumulibacter* at 2.5% and *Nitrosomonas* at 0.7%.

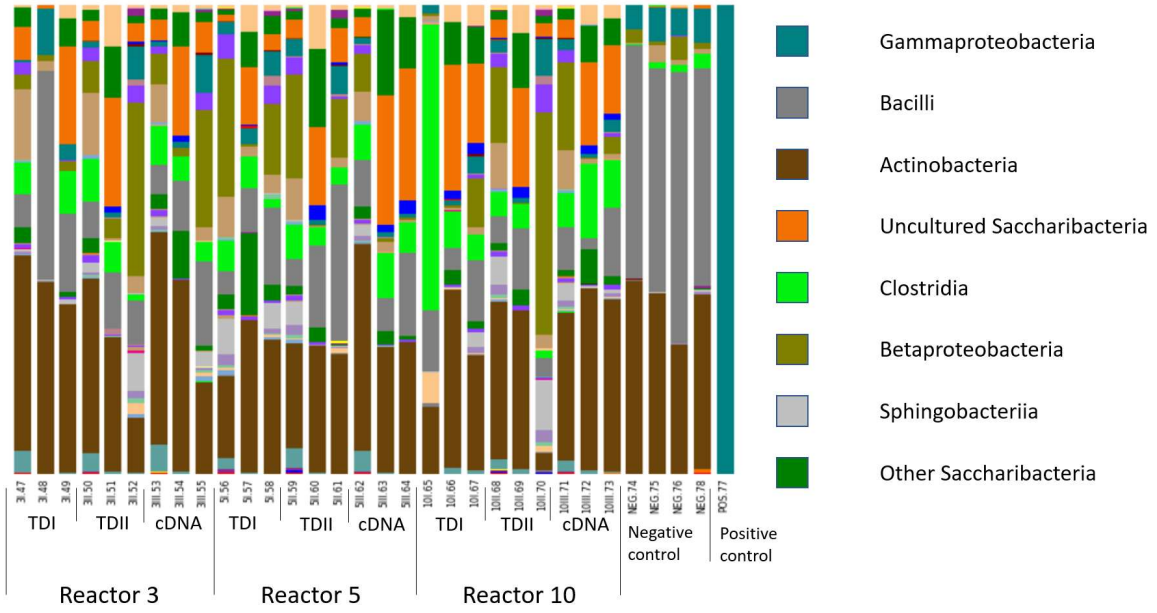

Figure 7: Bar plots for relative abundance of OTU from 16S RNA sequencing at class level. Size of bars corresponds to abundance of the OTU compared to others within the same parallel. Generated by the QIIME-pipeline. 3I.47 through 3III.55 are reactor 3, 5I.56 through 5III.64 are reactor 5, and 10I.65 through 10III.73 are reactor 10. Negative and positive controls are both displayed as well.

3.2.3. Differences in composition based on difference in reactors and treatment.

To make inferences about data, the twenty most abundant OTUs, not dominant in negative control samples, were selected. Figures 8 and 9 are diagrams showing average DNA abundance of the twenty selected OTUs across categories of reactors (3, 5 and 10) and sample treatment (TDI, TDII and cDNA). The genera are organized from left to right after the sum of relative quantity. All the diagrams show an approximation towards a one-tailed normal distribution, with the higher columns on the graph on the left side, then ebbing out towards the right. *Salinibacter, Tetrasphera, Pseudoclavibacter, Gulosibacter*, and *Leucobacter* are all in order actinobacteria, despite not being filtered out as negative controls. None of the 20 most abundant are in order bacilli.

The RNA-TDI is the sample category with the most remaining DNA. Here is how relative abundance changed for the 20 selected OTUs between reactors for the RNA TDI treatment. *Uncultured Saccharibacter* lowers from 9.5% at reactor 3 to 5.6% at reactor 5 and then up high to 14.7% at reactor 10. *Salinibacterium* at reactor 3 is low at 6,6%, goes to a higher 11,6% at reactor 5, goes down to 9,2% for reactor 10. *Tetrasphaera* starts high at 8,6% for reactor 3, goes down to 3,2% in reactor 5, and down again to 0.1% in reactor 10. *Other Saccharibacteria* goes from 3.4% at reactor 3, to 4.1% at reactor 5 and up again to 5.6% at reactor 10. *Gulosibacter* remains stable between reactor 3 and 5, then goes from 2.1% to 4.1% for reactor 10. For *Candidatus Accumulicbacter*, reactor 10 to 3 remain similar and at

reactor 5, 0.3% changes to 6.6%. *Unculutred Thermomicrobia* at reactor 10 to 3 remain similar, but at reactor 5, 14% changes to 7.9%.

Uncultured Ruminococcaea at reactor 3 at 1.4% changes to 0.7 % at reactor 5, then goes up to 3.6% at reactor 10, which is statistically significant. *Other Rhodobacteraceae* goes down from reactor 3 at 2.0% to 1.4% at reactor 5 and down again to 0.1% at reactor 10. For *Uncultured Comamonadacea*, reactor 10 to 3 remain similar, but at reactor 5, 0.1% changes to 1.2%. *Hydrogenophaga* remains stable between reactor 5 and 10 but goes down from 0.8% to 0.1% at reactor 3. *Uncultured Candidatus Saccharibacteria Bacterium* remains stable between reactor 3 and 5 but goes up from 0.1% to 1.4% at reactor 10. For *Nitrosomonas*, reactor 10 to 3 remain similar, but at reactor 5, 0.5% changes to 1.5%. Abundance in *Eubacterium Rectale Group* remains stable between reactor 3 and 5 but goes up from 0.1% to 4.5% at reactor 10. *Acetobacterium* goes from 0.4% at reactor 3 to a higher 0.6% at reactor 5, then down lower than 3 at 0.0% for reactor 10. *NS11-12 Marine group* remains stable between reactor 5 and 10, then drops from 0.6% to 0.1% for reactor 3. *Pseudoclavibacter, Leucobacter* and *Christencenella R-7* have relatively stable relative abundances, averaging at 3.2%, 1.1% and 0.7% respectively.

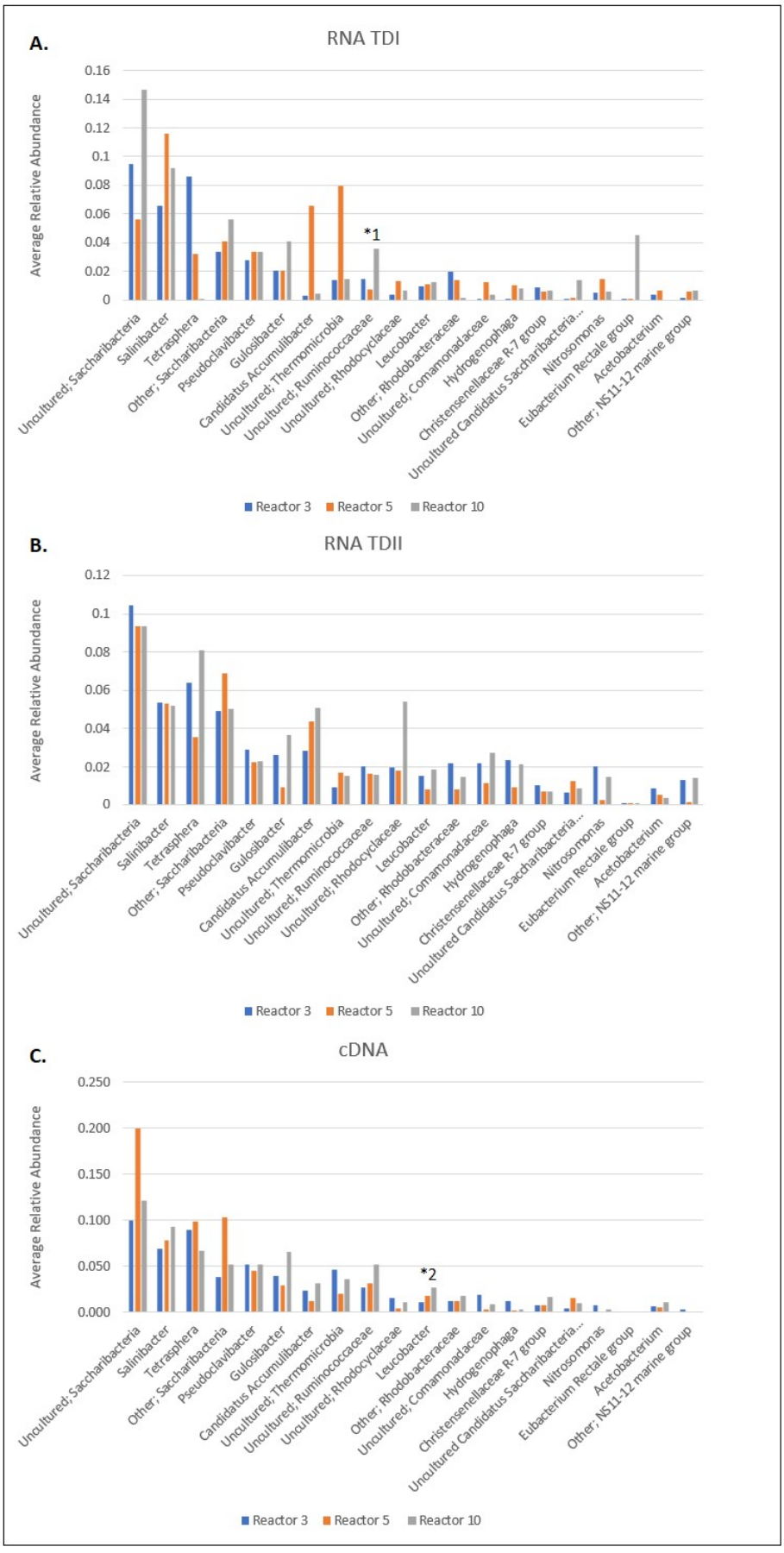
A.
RNA TDI
Average Relative Abundance
0.16
0.14
0.12
0.1
0.08
0.06
0.04
0.02
0
*1
Uncultured; Saccharibacteria
Salinibacter
Tetrasphera
Other; Saccharibacteria
Pseudoclavibacter
Gulosibacter
Candidatus Accumulibacter
Uncultured; Thermomicrobia
Uncultured; Ruminococcaceae
Uncultured; Rhodocyclaceae
Leucobacter
Other; Rhodobacteraceae
Uncultured; Comamonadaceae
Hydrogenophaga
Christensenellaceae R-7 group
Uncultured Candidatus Saccharibacteria...
Nitrosomonas
Eubacterium Rectale group
Acetobacterium
Other; NS11-12 marine group
Reactor 3
Reactor 5
Reactor 10
B.
RNA TDII
Average Relative Abundance
0.12
0.1
0.08
0.06
0.04
0.02
0
Uncultured; Saccharibacteria
Salinibacter
Tetrasphera
Other; Saccharibacteria
Pseudoclavibacter
Gulosibacter
Candidatus Accumulibacter
Uncultured; Thermomicrobia
Uncultured; Ruminococcaceae
Uncultured; Rhodocyclaceae
Leucobacter
Other; Rhodobacteraceae
Uncultured; Comamonadaceae
Hydrogenophaga
Christensenellaceae R-7 group
Uncultured Candidatus Saccharibacteria...
Nitrosomonas
Eubacterium Rectale group
Acetobacterium
Other; NS11-12 marine group
Reactor 3
Reactor 5
Reactor 10
C.
cDNA
Average Relative Abundance
0.250
0.200
0.150
0.100
0.050
0.000
*2
Uncultured; Saccharibacteria
Salinibacter
Tetrasphera
Other; Saccharibacteria
Pseudoclavibacter
Gulosibacter
Candidatus Accumulibacter
Uncultured; Thermomicrobia
Uncultured; Ruminococcaceae
Uncultured; Rhodocyclaceae
Leucobacter
Other; Rhodobacteraceae
Uncultured; Comamonadaceae
Hydrogenophaga
Christensenellaceae R-7 group
Uncultured Candidatus Saccharibacteria...
Nitrosomonas
Eubacterium Rectale group
Acetobacterium
Other; NS11-12 marine group
Reactor 3
Reactor 5
Reactor 10

Figure 8: Displays the average relative RNA-TDI (A), RNA-TDII (B) and cDNA (C) abundance of the twenty most abundant genera. The genera are organized by the sum of the abundances from highest on the left to lowest on the right. *1 is reactor 10 having significantly higher relative abundance of TDI RNA than reactor 5 for the *uncultured Ruminococcaceae*. *2 is reactor 10 having significantly higher relative cDNA abundance than reactor 5 for *Leucobacter.*

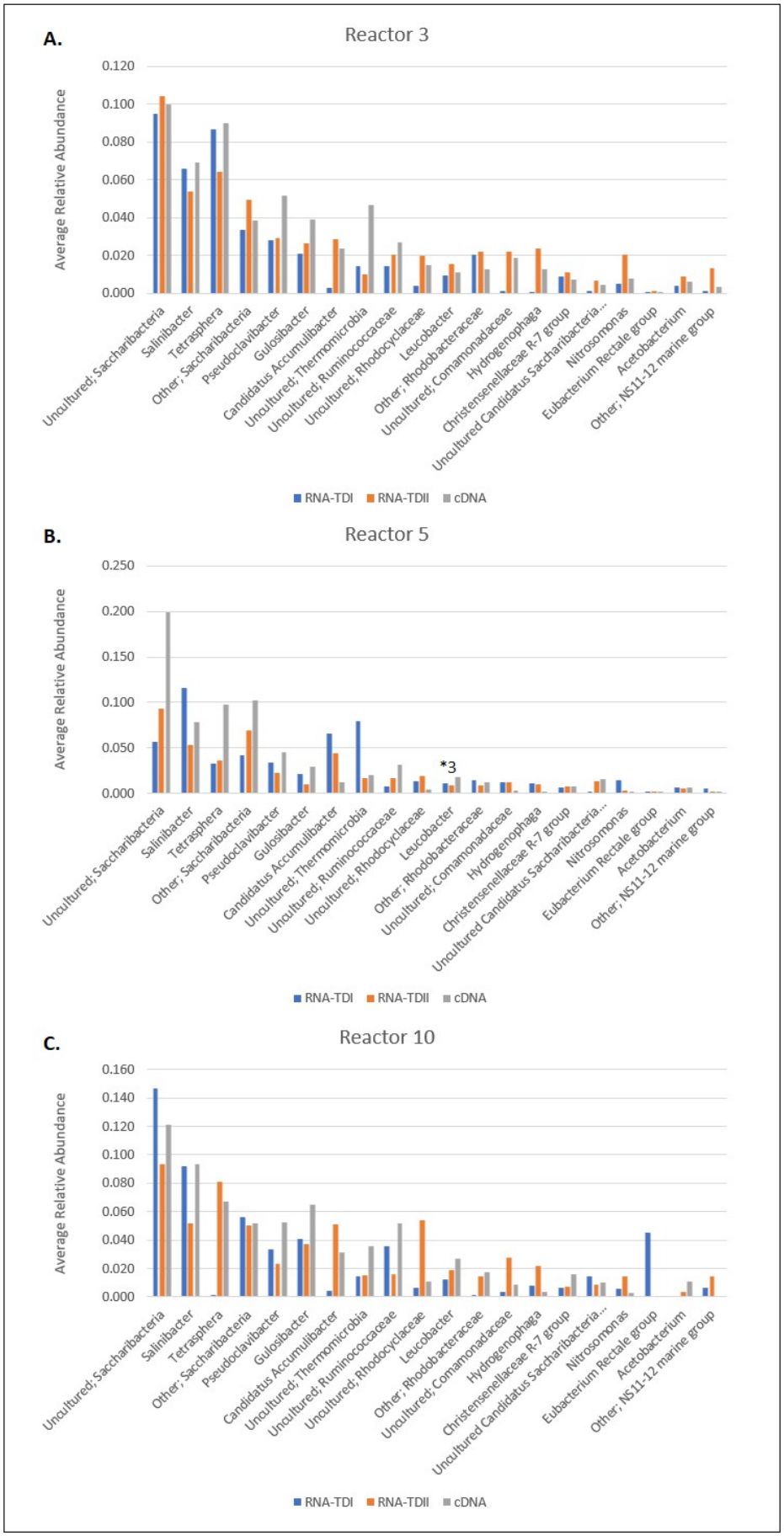
A.
Reactor 3
Average Relative Abundance
0.120
0.100
0.080
0.060
0.040
0.020
0.000
Uncultured; Saccharibacteria
Salinibacter
Tetrasphera
Other; Saccharibacteria
Pseudoclavibacter
Gulosibacter
Candidatus Accumulibacter
Uncultured; Thermomicrobia
Uncultured; Ruminococcaceae
Uncultured; Rhodocyclaceae
Leucobacter
Other; Rhodobacteraceae
Uncultured; Comamonadaceae
Hydrogenophaga
Christensenellaceae R-7 group
Uncultured Candidatus Saccharibacteria...
Nitrosomonas
Eubacterium Rectale group
Acetobacterium
Other; NS11-12 marine group
RNA-TDI
RNA-TDII
cDNA
B.
Reactor 5
Average Relative Abundance
0.250
0.200
0.150
0.100
0.050
0.000
*3
Uncultured; Saccharibacteria
Salinibacter
Tetrasphera
Other; Saccharibacteria
Pseudoclavibacter
Gulosibacter
Candidatus Accumulibacter
Uncultured; Thermomicrobia
Uncultured; Ruminococcaceae
Uncultured; Rhodocyclaceae
Leucobacter
Other; Rhodobacteraceae
Uncultured; Comamonadaceae
Hydrogenophaga
Christensenellaceae R-7 group
Uncultured Candidatus Saccharibacteria...
Nitrosomonas
Eubacterium Rectale group
Acetobacterium
Other; NS11-12 marine group
RNA-TDI
RNA-TDII
cDNA
C.
Reactor 10
Average Relative Abundance
0.160
0.140
0.120
0.100
0.080
0.060
0.040
0.020
0.000
Uncultured; Saccharibacteria
Salinibacter
Tetrasphera
Other; Saccharibacteria
Pseudoclavibacter
Gulosibacter
Candidatus Accumulibacter
Uncultured; Thermomicrobia
Uncultured; Ruminococcaceae
Uncultured; Rhodocyclaceae
Leucobacter
Other; Rhodobacteraceae
Uncultured; Comamonadaceae
Hydrogenophaga
Christensenellaceae R-7 group
Uncultured Candidatus Saccharibacteria...
Nitrosomonas
Eubacterium Rectale group
Acetobacterium
Other; NS11-12 marine group
RNA-TDI
RNA-TDII
cDNA

Figure 9: Displays the average relative RNA-TDI, RNA-TDII and cDNA abundance of the twenty most abundant genera in reactor 3 (A), 5 (B) and 10 (C). The genera are organized by the sum of the abundances from highest on the left to lowest on the right. *3 is *Leucobacter* having significantly higher relative abundance of cDNA than DNA TDII in reactor 5.

T-tests for checking statistically significant difference between different reactors for each OTU was conducted to check how RNA levels alongside the varying conditions of the reactors. For TDI RNA, only one comparison crossed the $\alpha = 0.05$ threshold. Reactor 5 against 10 for the *uncultured Ruminococcaceae* had a t-value of 0.029 at TDI. *Leucobacter* had significantly higher reactor 10 relative abundance than for reactor 5 with the cDNA treatment, with a t-value of 0.015.

T-tests were conducted based on determining statistical significance for DNA levels comparing the difference between cDNA levels and remaining DNA. *Leucobacter* was the only OTU that was statistically significantly high enough to pass the $\alpha = 0.05$ threshold, at a t-value of 0.037, for having a significantly higher amount of cDNA than TD-II DNA in reactor 5.

The small and highly variable abundances of RNA in each category and even among replicates makes the T-test show few comparisons within the threshold.

The RNA-TDI chart in figure 8 show some genera with variability between reactors. Only a few towards the low end of the distribution seem to be similar between reactors. *Tetrasphaera* has high levels of RNA in reactor 3, the *Uncultured Thermomicrobia* and *Candidatus Accumulibacter* has high levels for reactor 5, and *Eubacterium Rectale Group* and the *Uncultured Saccharibbacteria* has high levels in reactor 10.

On the RNA-TDII chart there is fewer differences between reactors for more genera. The *uncultured Rhodocycleae* is an outlier for reactor 10 for being higher and *Tetrasphaera* for being lower in reactor 5.

The cDNA diagram also looks more even than RNA-TDI. The *uncultured Saccharibacteria* and the other *Saccharibacteria* have outliers in reactor 5.

Figure 9 shows difference between the categories of sample treatments for the different reactors. In almost all these, the RNA-TDI and RNA-TDII levels are different. Sometimes there is more RNA-TDI, other times less. The differences can be very notable, like *Tetrasphaera* and *Eubacterium Rectale-group* for reactor 10.

cDNA levels have occasional outlier across figure 9. The *uncultured Thermomicrobia* for reactor 3, *uncultured Saccharibacteria* and *Tetrasphaera* for reactor 5. These are much higher than the TDI and TDII averages.

3.2.4. Functional assignment through MiDAS database

The twenty selected OTUs were checked against MiDAS field guide database. Only six of them, *Tetrasphaera, Candidatus Acuumulibacter, Leucobacter, Hydrogenophaga, Acetobacteria* and *Nitrosomonas* had an entry. Data regarding whether the genera contained organisms which were polyphosphate accumulating, nitrite reducing, ammonia to nitrite oxidizing, fermenting, aerobic heterotrophs, or chemoautotrophs. These six's substrate specificity is summarized in table 3.

Tetrasphaera and *Candidatus Accumulibacter* were both aerobic heterotroph polyphosphate accumulating organisms. These were also the most abundant genera out of the six. *Tetrasphaera* is the third most abundant genera among the twenty and *Candidatus Accumulibacter* is the seventh. *Leucobacter* is also an aerobic heterotrophic bacterium.

Nitrosomonas has both nitrite reducing capabilities as well as ammonium to nitrite oxidizing capabilities. This gives *Nitrosomonas* the ability to catalyze ammonium all the way to nitrogen gas or nitrous oxide. *Candidatus Accumulibacter, Leucobacter* and *Hydrogenophaga* can oxidize nitrite variably. Only *Acetobacteria* can definitively derive energy through fermentation among these genera, while being able to use chemoautotrophy. Both *Nitrosomonas* and *Hydrogenophaga* are mixotrophs.

Table 3: Nutrients as substrates for genera from the 16S analysis. The selection is from the twenty most abundant OTUs, determined by taking the sum of all raw data entries and filtering out the ones with negative value averages higher than any one reactor's average abundance. Out of these the table displays those genera which had an entry in the MiDAS database. The table is organized after relative abundance with the most abundant at the top and descending. The reactor columns are relative abundance of cDNA.

Genera	Reactor 3 DNA	Reactor 3 cDNA	Reactor 5 DNA	Reactor 5 cDNA	Reactor 10 DNA	Reactor 10 cDNA	PAO	Nitrite reduction	AOB	Fermentation	Aerobic heterotroph	Chemoautotroph
Tetrasphaera	0.086 (±0.122)	0.090 (±0.126)	0.032 (±0.045)	0.098 (±0.138)	0.001 (±0.001)	0.067 (±0.091)	Yes			Variable	Yes	
Candidatus Accumulibacter	0.003 (±0.004)	0.024 (±0.020)	0.066 (±0.074)	0.012 (±0.015)	0.004 (±0.006)	0.031 (±0.041)	Yes	Variable			Yes	
Leucobacter	0.009 (±0.011)	0.011 (±0.008)	0.011 (±0.003)	0.018 (±0.003)	0.013 (±0.011)	0.027 (±0.001)		Variable			Yes	
Hydrogenophaga	0.001 (±0.001)	0.012 (±0.015)	0.010 (±0.010)	0.002 (±0.002)	0.008 (±0.011)	0.003 (±0.003)		Variable			Yes	Yes
Nitrosomonas	0.005 (±0.005)	0.008 (±0.009)	0.015 (±0.020)	0.001 (±0.001)	0.006 (±0.008)	0.003 (±0.002)		Yes	Yes		Yes	Yes
Acetobacterium	0.004 (±0.005)	0.006 (±0.008)	0.006 (±0.006)	0.006 (±0.006)	0.000 (±0)	0.011 (±0.007)				Yes		Yes

4. Discussion:

4.1 Biological interpretation of data

4.1.1 TD-1 Abundance

Pseudoclavibacter, Leucobacter and *Christencenellacaea R-7* showed stable amounts of relative TD-I DNA abundance. Since *Pseudoclavibacter* and *Leucobacter* are both aerobic heterotrophic, one can infer they would have higher abundance in reactor 5 and 10 than reactor 3 (Manaia, 2004) (Takeuchi, 1996). *Christencenellacaea R-7* is an anaerobic fermentative heterotroph, for which higher abundance in reactor 3 is expected, rather than reactors 5 or 10 (Morotomi, 2012). *Peudoclavibacter* and *Christencenellacaea R-7* remain relatively stable in TD-II DNA relative amounts, but *Leucobacter* has a statistically significantly higher amount of abundance in reactor 10 than 5, with reactor 3 in between. High abundance in reactor 10 for *Leucobacter* can be explained through aerobic conditons, but the fact that reactor 5 abundance is lower than the anaerobic reactor 3 does not correspond with that.

There are three OTUs of *Saccharibacteria*: *uncultured Saccharibacter*, *other Saccharibacter* and *uncultured Candidatus Saccharibacteria bacterium*. These all have their highest relative abundance in reactor 10. This could be explained with these being aerobic heterotrophs, but some *Saccharibacter* can also catabolize glucose in anaerobic conditions. In cDNA abundance of all three, reactor 5 had the highest amount of cDNA. This could be explained through adaptation to the aerobic environment from living anaerobically. (Kindaichi, 2016)

The *uncultured Saccharibacter* is the most abundant OTU from the selection of 20 made in the results, at 9.5% relative abundance. Whether or not the *Saccharibacter* have any substrate specific importance to WTTP operation is unknown. Some *Saccharibacter* forms filaments. In the Nielsen 2010 study, almost 30% of abundance constituted filamentous bacteria. The *uncultured Saccharibacter* could therefore be filamentous, but further research would be needed to determine that.

Salinibacteria, Thermomicrobia and *Eubacterium Rectale* are aerobic heterotrophs. *Salinibacter* had its lowest abundance in reactor 3, had its highest relative abundance at the introduction of air in reactor 5 and remained high through to reactor 10 as expected. *Uncultured Thermomicrobia* also shows low abundance at reactor 3 to high one at reactor 5, but then goes down again to a lower level for reactor 10. *Eubacterium Rectale* only shows high abundance in reactor 10, as well as low levels across cDNA and TD-II DNA. (Karcher, 2020) (Han, 2003) (Hugenholtz, 2004)

Gulosibacter and *Comamonadaceae* are aerobic heterotrophs for which some strains can use nitrate as a terminal acceptor in respiration. *Guloibacter* showed stable abundance between reactor 3 and 5 then increases at reactor 10. High relative abundance in reactor 10 could be explained through aerobic conditions. *Uncultured Comamonadaceae* has low amounts of abundance in reactor 3 and 10 and peaks at reactor 5, while the opposite is true for cDNA levels. High abundance in reactor 5 could be explained

by *uncultured Comamonadaceae* being an aerobic bacterium, however the low abundance in reactor 10 does not fit that explanation. (Manaia, 2004) (Jara, 2018)

Ruminococcacaea and *Acetobacteria* are anaerobic fermentative bacteria. Abundance of *uncultured Ruminococcacaea* goes down between anaerobic reactor 3 and aerobic reactor 5 as explained through being anaerobic, but then has its highest relative abundance at 10, an amount which is statistically significantly larger. *Acetobacterium* shows a slight increase in relative abundance from reactor 3 to 5 but goes down to close to zero at reactor 10. (Rajilic-Stojanovic, 2014) (Balch, 1977)

Uncultured Rhodocyclaeae has its highest relative abundance in reactor 5, with reactor 3 showing slightly lower levels than reactor 10. *Rhodocyclaeae* can be photoautotrophic, photoheterotrophic, or chemoheterotrophic. Considering the high abundance in reactor 5, it could be a heterotrophic species. From graphical representation of the abundances, the *uncultured Rhodocyclaeae* appears like the *Candidatus Accumulibacter*, which is in the *Rhodocyclaeae* family. The *uncultured Rhodocyclaeae* could have the same substrate dependance and even phosphate binding as *Candidatus Accumulibacter*. More investigation would be needed to determine this. (Boden, 2017) (Fan, 2020)

Tetrasphaera is the third most abundant of the OTUs in the 20 OTU selection. This makes it the most abundant identified PAO in this dataset. In reactor 3, *Tetrasphaera* shows an average abundance of 8.6%, which goes down to 3.2% average at reactor 5, and down to 0.1% in reactor 10. *Tetrsphaera* is a heterotroph that can reduce nitrite or use oxygen gas. It therefore looks these observations like *Tetrasphaera* was most successful in the anaerobic chamber while expending their phosphorus reserves. (Maszenan, 2000)

Candidatus Accumulibacter is the second most abundant PAO OTU in the dataset. It has its highest abundance in reactor 5 with 6.6%, while reactors 3 and 10 are at around 0.3%. It shows the least amount of abundance of cDNA in reactor 5 as well. *Candidatus Accumulibacter* derives energy from organic carbon sources, and can use nitrate, nitrite, or oxygen as electron acceptors for its respiration. The distribution of relative abundances across reactors for *Candidatus Accumulibacter* is not like *Tetrasphaera*. The only other OTU with a similar relative abundance spread among the 20 abundant OTUs would be the *Uncultured Thermomicrobia*, which also shows a much higher abundance in reactor 5 than in the other reactors. (Fan, 2020)

Hydrogenophaga has environmentally dependent nitrite reduction. It is an aerobic chemoorganotroph and facultative chemolithoautotrophic species. It has a low abundance of 0.1% in reactor 3 and a higher one of 0.8% in reactor 5 and 10. (Kämpfer, 2005)

Nitrosomonas is an autotroph that can oxidize ammonia to nitrite and reduce nitrite. This makes it important for the SND process of the WTTP. It can also help in establishing biofilm. *Nitrosomonas* shows a low relative abundance in reactor 3 and 10, which then goes from 0.005 to 0.015 from reactor 3 to 5. This pattern of abundance is like *Candidatus Accumulibacter*, but with lesser magnitude of difference between the reactors. (Chawley, 2020)

NS11-12 Marine group has a low abundance in reactor 3, before going up for reactor 5 and remains stable to reactor 10. No available literature on the nutrition or biochemistry of this OTU.

GAOs are known to hinder optimization of EBPR. No known GAO was among the 20 most abundant OTUs. Four common GAOs in *Competibacter, Contendibacter, Defluviicoccus* and *Thioalkanivibrio* were scanned for in the sequencing data to assess relative abundance. *Competibacter* was found at 0.1% relative abundance in the data set. *Contendibacter, Defluviicoccus* and *Thioalkanivibrio* gave no hits when searched for, it is therefore reasonable to assume they are not present.

4.1.2 rRNA Abundance

The qubit measurements of cDNA, rRNA, showed amounts of nucleic acid below the detection limit. Reactor 5 *Uncultured Saccharibacter* has the highest average value of any of the nucleic acids across all treatments in the selection of 20. The *Other Saccharibacter* and the *uncultured Candidatus Saccharibacter* has their highest average relative abundance in reactor 5. *Salinibacter, Leucobacter* and the *uncultured Rhodocyclaceaes* abundance increases between reactor 3 and 5 and between reactor 5 and 10. *Tetrasphaera* has a higher relative abundance in reactor 3 than 10, with its highest at reactor 5. *Candidatus Accumulibacter* has its highest abundance in reactor 10, with the lowest in reactor 5. *Nitrosomonas* has its highest abundance in reactor 3 and its lowest in reactor 5. The difference in abundance between reactor 10 and 5 in *Leucobacter* is statistically significant.

4.2 Methodological considerations and limitations:

Sources in environmental nucleic acid isolation are limited based on examination of the literature. Methods for isolating RNA and DNA from cell samples as described in the literature is commonly for medical science purposes or non-aqueous, non-biofilm mediums. Some of the known issues of environmental nucleic acid extraction is discussed in the following paragraphs.

There are known PCR issues regarding capturing full diversity and in aqueous environmental systems. PCR and RT-PCR enzymes have been known to preform worse in water samples. Ions and contaminants like humic acids can inhibit the enzymes and prevent proper functioning. (Hill, 2015).

Shearing and cell lysis are important for improving the RNA isolation. The abundance is determined by the shear used. A high amount of stress during lysis might break open more cells across the entire biofilm, which could give a more representative selection of the diversity in the biofilm as well. High degree of lysis destroys nucleic acids too. Low shear means only surface microbes on the biofilm might be represented in the sequencing data. This potential skewedness could be worked around by introducing multiple levels of shear to further procedures. The variety of cells in environmental samples differ in terms of morphology, size, and cell wall composition, all of which affects ease of lysis and nucleic acid extraction (Mäki, 2017) As an example, gram positive bacteria are more resistant to chemical lysis, which effects nucleic acid effectiveness (Hill, 2015).

The cause of low amounts of nucleic acids and other related issues could come from a still unoptimized nucleic acid homogenization protocol. Only small amounts of nucleic acids were successfully isolated as seen from the gel images and qubit concentrations. However, as the positive controls showed higher levels of DNA in the test run assays, the issue is most likely with the homogenization step, and not with isolation of DNA. This is also why the isolation step was most changed during the process optimization. Based on the results, more optimization is needed. To achieve results with more nucleic acids, different types of cell lysis should be tested. For higher DNA in the samples, a parallel untreated by Turbo-DNase could be implemented and used for more accurate comparisons. Low RNA could come from RNase contamination, despite use of RNase away. More rigorous use of RNase is recommended. The use of TRIzol has also been suggested as an alternative to RNA-later for preserving RNA during storage.

For inferences about the results to hold solid ground, statistical backing is needed. There are large variations in the dataset, and it is uncertain whether this comes from natural causes or a technical issue. These variations give poor certainty to the biological connections and inferences with the data. The data set worked with showed large differences between relative abundances within the same reactors and treatments. In many cases the average values worked with only constituted one non-zero parallel or be associated with a high variance. The T-tests conducted show this lack of rigidity. One would expect OTUs with great variance between reactors to show as significantly different in a T-test. As an example, differences in averages between reactor 5 and 10 in cDNA for *Leucobacter* is much less than the differences in TD-I RNA for reactor 5 in *Candidatus Accumlibacter*, which was not statistically significant according to the T-test. Changing the α from 0.005 to 0.010 does not change this.

Increasing the number of parallels is a way to better statistical rigidity. Another way to increase the statistical certainty would be to make sure parallels within the same treatment and reactor had less variance. This unevenness could come from low nucleic acid amounts. When the amount of nucleic acid is small, natural variations in the samples will have a relatively greater impact, which increases variance.

4.3 Conclusion and further work:

The protocol yielded meta transcriptome data on the Hias process biofilm. The most abundant OTU was *uncultured Saccharibacter*, with the most abundant PAO being *Tetrasphaera* and the most abundant ammonia oxidizer being *Nitrosomonas*. The small amounts of nucleic acids and the lack of a non-DNase treated triplicate parallel contributed to a statistical uncertainty, which impacts ability to make inferences about the data. Further work is suggested to further optimize the protocol in nucleic acid extraction. Examples of this is more experimentation with different lysis methods, as well as ways to better preserve nucleic acids. TRIzol could be tested as an alternative to preserve RNA. To compare cDNA with total nucleic acid amount, it is recommended to have one parallel not treated with any DNase.

References:

Balch, W.E.; Schoberth, S.; Tanner, R.S.; Wolfe, R.S. (1977) *Acetobacterium,* a New Genus of Hydrogen-Oxidizing, Carbon Dioxide-Reducing, Anaerobic Bacteria. *International journal of systematic and evolutionary microbiology,* 24 (4)
URL: https://www.microbiologyresearch.org/docserver/fulltext/ijsem/27/4/ijs-27-4-355.pdf?expires=1625405102&id=id&accname=guest&checksum=76A571D9BCDBB99FD01D4992F2D52532

Bechmann, M.; Thrane, J-E.; Kværnø, S.; Turtumøygard, S. (2021) Eutrofiering av Mjøsa. *NIBIO Rapport,* 7 (58), pp 1 – 26.
URL: https://www.vassdragsforbundet.no/wp-content/uploads/2021/04/Eutrofi_Mj%C3%B8sa_NIBIO_2021.pdf

Bhagowati, B.; Ahamad, K. U. (2018) A review on lake eutrophication dynamics and recent developments in lake modeling. *Ecohydrology and hydrobiology,* volume 10, issue 1, pp 155-166
URL: https://www.sciencedirect.com/science/article/pii/S164235931730143X

Boden, R.; Hutt, L.P.; Rae, A.W. (2017) Reclassification of Thiobacillus aquaesulis (Wood & Kelly, 1995) as *Annwoodia aquaesulis gen. nov., comb. nov.,* transfer of *Thiobacillus* (Beijerinck, 1904) from the *Hydrogenophilales* to the *Nitrosomonadales*, proposal of *Hydrogenophilalia class. nov*. within the '*Proteobacteria'*, and four new families within the orders *Nitrosomonadales* and *Rhodocyclales*. *International journal of systematic and evolutionary microbiology,* 67 (5)
URL: https://www.microbiologyresearch.org/content/journal/ijsem/10.1099/ijsem.0.001927

Buermans, H.P.J.; den Dunnen, J.T. (2014) Next generation sequencing technology: Advances and applications. *Biochemica et biophysica Acta – Molecular basis of disease.* 1842 (10): 1932 -1941
URL: https://www.sciencedirect.com/science/article/pii/S092544391400180X

Bunce, J.T.; Ndam, E.; Ofiteru, I.D.; Moore, A.; Graham, D.W. (2018) A Review of Phosphorus Removal Technologies and Their Applicability to Small-scale domestic wastewater treatment systems. *Frontiers in Environmental Sciences,* 6 (8).
URL: https://www.frontiersin.org/articles/10.3389/fenvs.2018.00008/full

Caparaso, J.G.; Kuczynski, J.; Stombaugh, J.; Bittinger, K.; Bushman, F.D.; Costello, E.K.; Fierer, N.; Pena, A.G.; Goodrich, J.K.; Gordon, J.I.; Huttley, G.A.; Kelley, S.T.; Knights, D.; Koening, J.E.; Ley, R.E.; Lozupone, C.A.; McDonald, D.; Muegge, B.D.; Pirrung, M.; Reeder, J.; Sevinsky, J.R.; Turnbaugh, P.J.; Walters, W.A.; Widmann, J.; Yatsunenko, T.; Zaneveld, J.; Knight, R. (2010) What is QIIME? *Nature Methods.*
URL: http://qiime.org/

Chawley, P.; Banerjee, C.; Jagadevan, S. (2020) Growth of planktonic and biofilm culture of *Nitrosomonas mobilis* Ms1 in response to stoichiometric ammonia consumption. *International biodetrioration & Biodegredation,* 154.
URL: https://www.sciencedirect.com/science/article/pii/S0964830520305394

Di Biase, A.; Kowalski, M. S.; Devlin, T. R.; Oleszkiewicz, J. A. (2019) Moving bed biofilm reactor technology in municipal wastewater treatment: A review. *Journal of environmental management,* 247: 849-866.
URL: https://www.sciencedirect.com/science/article/pii/S0301479719308448#sec3

Donlan, R.M. (2002) Biofilms Microbial Life on Surfaces. *Emerging infectious diseases,* 8 (9): 881 – 890.
URL: https://www.ncbi.nlm.nih.gov/pmc/articles/PMC2732559/

Fan, Z.; Zeng, W.; Wang, B.; Guo, W.; Meng, G.; Peng, Y. (2020) Transcriptional responses of *Candidatus Accumulibacter* clades to environmental dynamics in enhanced biological phosphorus removal. *Bioresource Technology,* volume 306
URL: https://www.sciencedirect.com/science/article/pii/S0960852420303771

Green, M.R.; Sambrook, J. (2019) How to win battles against RNases. *Cold spring harbor laboratory press.*
URL: http://cshprotocols.cshlp.org/content/2019/2/pdb.top101857.long

Han, S.K.; Nedashkovskaya, O.I.; Mikhailov, V.V.; Kim, Seung, B.K.; Bae, K.S. (2003) *Salinibacterium amurskyende* gen. nov. sp. Nov., a novel genus of the family *Microbacteriaceae* from the marine environment. *International Journal of systematic and evolutionary microbiology*, 53 (6)
URL: https://www.microbiologyresearch.org/content/journal/ijsem/10.1099/ijs.0.02627-0#tab2¨

Hias (2021) The Hias®-process.
URL: https://www.hias.as/

Hill, V.R.; Narayanan, J.; Gallen, R.R.; Ferdinand, K.L.; Cromeans, T.; Vinjé, J. (2015) Development of a nucleic acid extraction procedure for simultaneous recovery of DNA and RNA from Microbes in water. *Pathogens,* 4 (2).
URL: https://www.mdpi.com/2076-0817/4/2/335/htm

Hreiz, R.; Laifi, MA; Roche, N. (2015) Optimal design and operation of activated sludge processes: State-of-the-Art. *Chemical Engineering journal,* 281: 900-920.
URL: https://www.sciencedirect.com/science/article/pii/S1385894715009766

Hugenholtz, P.; Stackebrandt, E. (2004) Reclassification of *Sphaerobacter termophilus* from the subclass *Sphaerobacteridae* in the phylum *Actinobacteria* to the class *Thermomicrobia* (emended description) in the phylum *Chloroflexi* (emended description). *International Journal of systematic and evolutionary microbiology*, 54 (6).
URL: https://www.microbiologyresearch.org/content/journal/ijsem/10.1099/ijs.0.03028-0

Invitrogen (2018) MagMAX-96 for Micorarrays Total RNA Isolation Kit
URL: https://www.thermofisher.com/document-connect/document-connect.html?url=https%3A%2F%2Fassets.thermofisher.com%2FTFS-Assets%2FLSG%2Fmanuals%2F1839M_MgMAX96Microarys_UG.pdf

Jara, E.; Morel, M.A.; Lamolle, G.; Castro-Sowinski, S.; Simón, D.; Iriarte, A.; Musto, H. (2018) The complex pattern of codon usage evolution in the family Comamonadaceae. *Ecological Genetics and genomics,* 6: . 1 – 8.
URL: https://www.sciencedirect.com/science/article/pii/S2405985417300277

Kämpfer, P.; Schilze, R.; Jäckel, U.; Malik, K.A.; Amann, R.; Spring, S. (2005) *Hydrogenophaaga defluvi* sp. Nov. and *Hydrogenophaga atypica* sp. Nov. isolated from active sludge. *International journal of systematic and evolutionary microbiology,* 55 (1): 341 – 344.
URL: https://pubmed.ncbi.nlm.nih.gov/15653898/

Karcher, N.; Pasolli, E.; Asnicar, F.; Huang, K.D.; Tett, A.; Manara, S.; Armanini, F.; Bain, D.; Duncan, S.H.; Louis, P.; Zolfo, M.; Manghi, P.; Valles-Colomer, M.; Raffaeta. R.; Rota-Stabelli, O.; Collado, M.C.; Zeller, G.; Falush, D.; Maixner, F.; Walker, A.W.; Huttenhower, C.; Segata, N. (2020) Analyis of 1321 *Eubactrium rectale* genomes from metagenomes uncovers complex phylogeographic population structure and subspecies functional adaptations. *Genome biology,* 21 (138).
URL: https://genomebiology.biomedcentral.com/articles/10.1186/s13059-020-02042-y

Kindaichi, T.; Yamaoka, S.; Uehara, R.; Ozaki, N.; Ohashi, A.; Albertsen, M.; Nielsen, P.H.; Nielsen, J.L. (2016) Phylogenetic diversity and ecophysiology of Candidate phylum *Saccharibacteria* in activated sludge. *FEMS Microbiology Ecology*, 92 (6)
URL: https://academic.oup.com/femsec/article/92/6/fiw078/2470075?login=true

Lenntech (2021) Phosphorus removal.
URL: https://www.lenntech.com/phosphorous-removal.htm

Mäki, A.; Salmi, P.; Mikkonen, A.; Kremp, A.; Tiirola, M. (2017) Sample Perservation, DNA or RNA Extraction and Data Analysis for High-Throughput Phytoplankton Community Sequencing. *Frontiers in Microbiology.*
URL: https://www.frontiersin.org/articles/10.3389/fmicb.2017.01848/full#B17

Manaia, C.M.; Nogales, B.; Weiss, N.; Nunes, O.C. (2004) *Gulosibacter molinativorax* gen. nov., sp. Nov., a molinate- degrading bacterium and classification of '*Brevibacterium helvolum'* DSM 20419 as *Pseudoclavibacter helvolus* gen. nov., sp. nov. . *International Journal of systematic and evolutionary microbiology*, 54 (3).
URL: https://www.microbiologyresearch.org/content/journal/ijsem/10.1099/ijs.0.02851-0?crawler=true

Maszenan, A.M.; Seviour, R.J.; Patel, B.K.; Schumann, P.; Burghardt, J.; Tokiwa, Y.; Stratton, H.M. (2000) Three isolates of novel polyphosphate-accumulating gram-positive cocci, obtained from activated sludge, belong to a new genus, *Tetrasphaera* gen. nov. and description of two new species, *Tetrasphaera japonica* sp. Nov. and *Tetrasphaera australiensis* sp. Nov. *International Journal of systematic and evolutionary microbiology*, 50 (2).
URL:
https://www.microbiologyresearch.org/docserver/fulltext/ijsem/50/2/0500593a.pdf?expires=1625390980&id=id&accname=guest&checksum=894679CF129329AF024FDF65AC2582BA

Morotomi, M.; Nagai, F.; Watanabe, Y. (2012) Description of *Christensenella minuta* gen. nov., sp. nov., isolated from human faeces, which forms a distinct branch in the order *Clostridiales*, and proposal of *Christensenellaceae* fam. nov. *International journal of systematic and evolutionary microbiology,* 62 (1)
URL: https://www.microbiologyresearch.org/content/journal/ijsem/10.1099/ijs.0.026989-0

Nielsen, P. H.; Mielczarek, A. T.; Kragelund, C.; Nielsen, J. L.; Saunders, A. M.; Kong, Y.; Hansen, A. A.; Vollertsen, J. (2010) A conceptual ecosystem model of microbial communities in enhanced biological phosphorus removal plants. *Water research,* 44 (17): 5070 – 5088.
URL: https://www.sciencedirect.com/science/article/pii/S004313541000504X?via%3Dihub

Norwegian Ministry of environment (1979) The Mjøsa Campaign. *Status report.*
URL:
https://web.archive.org/web/20160309201237/http://fylker.miljostatus.no/Global/Hedmark/vannforurensning/Statusrapport_Mjosaksjonen_46sDS-file2668.pdf

Oehmen, A.; Lemos, P. C.; Carvalho, G.; Yuan, Z.; Keller, J.; Blackall, L. L.; Reis, M. A. M. (2007) Advances in enhanced biological phosphorus removal: From micro to macro scale. *Water research,* 41 (11): 2271 – 2300
URL: https://www.sciencedirect.com/science/article/pii/S0043135407001091

Pray, L. (2008) The biotechnology revolution: PCR and the use of reverse transcriptase to clone expressed genes. *Nature education,* 1(1): 94
URL: https://www.nature.com/scitable/topicpage/the-biotechnology-revolution-pcr-and-the-use-553/

Rajilic-Stojanovic, M.; de Mos, W.M. (2014) The first 1000 cultured species of the human gastrointestinal microbiota. *FEMS Microbiology reviews,* 38 (5): 996-1047
URL: https://www.ncbi.nlm.nih.gov/pmc/articles/PMC4262072/

Roy, S.; Guanglei, Q.; Zungia-Montanez, R.; Williams, R.B.H.; Wuertz, S. (2021) Recent advances in understanding the ecophysiology of enhanced biological phosphorus removal. *Current opinion in biotechnology,* 67: 166-174.
URL: https://www.sciencedirect.com/science/article/pii/S0958166921000161

Rudi, K.; Goa, I.A.; Saltnes, T.; Sørensen, G.; Angell, I.L.; Eikås, S. (2019) Microbial ecological processes in MBBR biofilms for biological phosphorus removal from wastewater. *Water science and technology,* 79 (8): 1467 – 1473
URL: https://iwaponline.com/wst/article/79/8/1467/66977/Microbial-ecological-processes-in-MBBR-biofilms

Rusten, B.; Eikebrokk, B.; Uglenes, Y.; Lygren, E. (2006) Design and operations of the Kaldnes moving bed biofilm reactors. *Aquacultural engineering,* 34 (3): 322 – 331.
URL: https://www.sciencedirect.com/science/article/pii/S0144860905000531

Ruttenberg, K. C. (2003) The Global Phosphorus Cycle, *Treatise on Geochemistry,* Volume 8: 585-643.
URL: https://faculty.uml.edu//david_ryan/84.653/documents/RuttenbergGlobalPCycle.pdf

Saltnes, T.; Sørensen, G.; Eikås, S. (2017) Biological nutrient removal in a continuous biofilm process. *Water Practice & Technology,* 12 (4): 797 - 805.
URL: https://iwaponline.com/wpt/article/12/4/797/38657/Biological-nutrient-removal-in-a-continuous

Seifi, M.; Fazaelipoor, M.H. (2012) Modeling simultaneous nitrification and denitrification (SND) in a fluidized bed biofilm reactor. *Applied Mathematical Modelling,* 36 (11): 5603 – 5613.
URL: https://www.sciencedirect.com/science/article/pii/S0307904X12000194

Takeuchi, M.; Weiss, N.; Schumann, P.; Yokota, A. (1996) *Leucobacter komagatae* gen. nov. sp. nov., a New Aerobic Gram-positive, Nonsporulating Rod with 2,4-diaminobutyric acid in the cell wall. *International journal of systematic and evolutionary microbiology,* 46 (4)
URL: https://www.microbiologyresearch.org/content/journal/ijsem/10.1099/00207713-46-4-967

Tarayre, C.; Nguyen, H.; Brognaux, A.; Delepierre, A.; De Clercq, L.; Charlier, R.; Michels, E.; Meers, E.; Delvigne, F. (2016) Characterisation of Phosphate Accumulating Organisms and Techniques for polyphosphate detection. *Sensors,* 16 (6): 797 -.
URL: https://www.mdpi.com/1424-8220/16/6/797/htm

Norges miljø- og biovitenskapelige universitet
Noregs miljø- og biovitskapelege universitet
Norwegian University of Life Sciences

Postboks 5003
NO-1432 Ås
Norway